Journal of Chromatography A, 1380 (2015) 146–155

Contents lists available at ScienceDirect

Journal of Chromatography A

journal homepage: www.elsevier.com/locate/chroma

Polysaccharide characterization by hollow-fiber flow field-flow fractionation with on-line multi-angle static light scattering and differential refractometry

Leena Pitkänen, André M. Striegel*

Chemical Sciences Division, National Institute of Standards and Technology (NIST), 100 Bureau Drive, MS 8392, Gaithersburg, MD 20899, United States

ARTICLE INFO

Article history:
Received 7 October 2014
Received in revised form 5 December 2014
Accepted 23 December 2014
Available online 3 January 2015

Keywords:
Hollow-fiber flow field-flow fractionation
Polysaccharides
Dextran
Pullulan
Arabinogalactan
Light scattering

ABSTRACT

Accurate characterization of the molar mass and size of polysaccharides is an ongoing challenge, oftentimes due to architectural diversity but also to the broad molar mass (M) range over which a single polysaccharide can exist and to the ultra-high M of many polysaccharides. Because of the latter, many of these biomacromolecules experience on-column, flow-induced degradation during analysis by size-exclusion and, even, hydrodynamic chromatography (SEC and HDC, respectively). The necessity for gentler fractionation methods has, to date, been addressed employing asymmetric flow field-flow fractionation (AF4). Here, we introduce the coupling of hollow-fiber flow field-flow fractionation (HF5) to multi-angle static light scattering (MALS) and differential refractometry (DRI) detection for the analysis of polysaccharides. In HF5, less stresses are placed on the macromolecules during separation than in SEC or HDC, and HF5 can offer a higher sensitivity, with less propensity for system overloading and analyte aggregation, than generally found in AF4. The coupling to MALS and DRI affords the determination of absolute, calibration-curve-independent molar mass averages and dispersities. Results from the present HF5/MALS/DRI experiments with dextrans, pullulans, and larch arabinogalactan were augmented with hydrodynamic radius (R_H) measurements from off-line quasi-elastic light scattering (QELS) and by R_H distribution calculations and fractogram simulations obtained via a finite element analysis implementation of field-flow fractionation theory by commercially available software. As part of this study, we have investigated analyte recovery in HF5 and also possible reasons for discrepancies between calculated and simulated results vis-à-vis experimentally determined data.

Published by Elsevier B.V.

1. Introduction

The heterogeneity of chain lengths that exists in polysaccharides translates into these possessing a distribution of molar masses. The breadth or narrowness of this molar mass distribution (MMD) controls processing and end-use properties such as digestibility, solubility, elongation, tensile strength, and adhesion [1]. Determination of the MMD of biomacromolecules is performed most readily through separation science, where size-exclusion chromatography (SEC) has emerged as the most prominent technique in this regard [2]. When coupled to "absolute" detection methods such as static light scattering (SLS) in combination with concentration-sensitive detection, determination of the MMD and accompanying statistical moments can be accomplished by SEC without relying on calibration curves or the need for well-characterized standards [3], the latter being non-existent for a number of important polysaccharides such as cellulose, chitin, etc. For polysaccharides such as dextran, pullulan, and arabinogalactan, the molar mass (M) and MMD have been found to influence the role these polymers play in coatings, adhesives, binders, plasma volume expanders, contact lenses, perfusion solutions for organ transplants, artificial sweeteners and, even, in the mining industry for the reverse floatation of iron ores [4].

As M increases, however, accurate polysaccharide characterization by SEC becomes more difficult due to the increased propensity for chain scission at longer chain lengths in conjunction with the large shear rates to which polymers are exposed within the chromatographic columns [5–7]. To overcome this propensity for degradation, which has been observed for, e.g., alternan and amylopectin [8,9], gentler separation techniques have been employed. Chief among these are hydrodynamic chromatography (HDC) and asymmetric flow field-flow fractionation (AF4), both in conjunction with multi-angle static light scattering (MALS) detection [10–14].

* Corresponding author.
E-mail address: andre.striegel@nist.gov (A.M. Striegel).

http://dx.doi.org/10.1016/j.chroma.2014.12.070
0021-9673/Published by Elsevier B.V.

In light of the above, it appears obvious that other low-shear separation methods are needed to accurately characterize polysaccharide molar mass. A relatively new technique that has emerged for characterizing proteins and particles is hollow-fiber flow field-flow fractionation (HF5). Originally pioneered by Lee et al. and further developed by Carlshof and Jönsson and by Kok and colleagues [15–17], HF5 is a liquid-phase separation method in which solvent (or carrier medium, in the case of particle analysis) flows longitudinally and laminarly through a porous fiber sealed inside a plastic housing. Mechanically generated suction along the main fiber axis generates a cross flow perpendicular to the main solvent flow. The combination of longitudinal and radial flows allows the focusing of analytes at the fiber walls and subsequent separation based on differences in the analytes' translational diffusion coefficients.

There are a number of advantages to utilizing HF5 for characterizing potentially labile polysaccharides. It is a gentler method than are SEC or HDC, due to the lower shear forces to which the analyte is exposed in HF5 as compared to within chromatographic columns. For a field-flow fractionation (FFF) method, HF5 can be considered as possessing relatively high efficiency as a result of the large plate numbers (relative to other FFF methods) generated within the fiber, while the low dilution that occurs in HF5 as a result of the low fiber volume as compared to, e.g., the higher volume of an AF4 channel, translates into a generally higher sensitivity in HF5 than in AF4 analyses. There is also a lower propensity for overloading and for analyte aggregation in HF5 as compared to AF4, due to the fact that the same retention can be achieved in the former using concentrations one-third lower than in the latter. (For a review of the principles of HF5, the reader is referred to Refs. [17–20]) The low sample load required in HF5 can also present a disadvantage, however, in terms of low signal-to-noise ratios (S/N) in detector outputs, though for *M*-sensitive detection methods such as multi-angle static light scattering (MALS), for a given concentration S/N will improve with increasing *M*.

The application of HF5 to polysaccharide analysis was first demonstrated by Wijnhoven et al. nearly 20 years ago [21], and has not been capitalized upon since. For their experiments, these authors constructed a system in-house consisting of polysulfone fibers, which were connected to the injector and to a UV detector by being glued with epoxy glue over poly-ether ether ketone tubes. The fibers were further inserted into a glass tube, which was suctioned to create the cross flow. In stark contrast, the HF5 system employed here utilizes polyethersulfone (PES) fibers which are robust, commercial-grade products manufactured to a high degree of reproducibility (it is notable that PES has been shown to be resistant to fouling by aqueous dextran solutions at the concentrations employed in HF5 experiments, and even at multiples thereof, as demonstrated in Ref. [20]) [22,23]. These low-cost materials allow for at least 100 runs per fiber cartridge, with the latter being both easily disposable and simple to install with minimal system downtime. Within the cartridges, the PES fibers are sealed glue-free within a poly(ethylene terephthalate) housing. The sealing mechanism, which is described in Ref. [24], can be adapted to a variety of fiber diameters. If this commercially available HF5 system can be applied successfully to the analysis of polysaccharides, it would extend the arsenal of techniques available for this purpose, without the need for in-house system construction and with the possibility for determining the *M* averages and MMDs of polysaccharides that currently elude accurate characterization.

To address the above, we have coupled a commercially available HF5 system on-line to both MALS and differential refractometry (DRI) detectors and employed this system to characterize a series of pullulans and dextrans, and also an arabinogalactan. We chose pullulans and dextrans as our primary test analytes, as these polysaccharides can generally be considered well-characterized and thus lend themselves to evaluating both the applicability of multi-detector HF5 to the study of polysaccharides and the accuracy of our experiments. (As such, the experiments presented here address not the indispensability of HF5 as a polysaccharide characterization technique but, rather, the applicability and accuracy of multi-detector HF5 in the study of polysaccharides of varying anomeric configuration and glycosidic linkage.) Results of the HF5/MALS/DRI determinations are augmented here both by off-line quasi-elastic light scattering (QELS) experiments and by simulations based on a combination of FFF theory and finite element analysis. We hope that the present study will open the door to widespread characterization of polysaccharides by HF5/MALS/DRI, especially for polysaccharides the MMD of which cannot be readily and/or accurately characterized by other means.

2. Materials and methods

2.1. Polysaccharide samples

Pullulans with nominal *M* (in g mol^{-1}) of 22,800, 212,000, 380,000, and 1,660,000 were all purchased from Agilent/Polymer laboratories (Amherst, MA). Molar mass dispersities ($Đ \equiv M_w/M_n$) given by the manufacturer for pullulans were 1.07, 1.13, 1.12, and 1.19, respectively. Dextrans with nominal *M* (in g mol^{-1}) of 50,000, 270,000, and 670,000 were from Fluka (Buchs, Switzerland), and dextran with nominal *M* of 3,500,000 g mol^{-1} was from PSS Polymer Standard Service (Mainz, Germany). Corresponding molar mass dispersities of dextrans were 1.36, 1.66, 2.01, and 2.50, respectively. Larch arabinogalactan (also known as arabinogalactan Type II) was from Atomergic Chemetals Corp. (6030), isomaltoheptaose from Seikagaku Corp. (Tokyo, Japan), and maltoheptaose from Sigma (Steinheim, Germany).

2.2. HF5/MALS/DRI analysis

The HF5 analyses were carried out using an Agilent 1260 isocratic HPLC pump (Agilent Technologies, Santa Clara, CA), a manual injector (High-Pressure Injection System, Wyatt Technology Co., Santa Barbara, CA), an Eclipse DualTec FFF control module (Wyatt Technology Co.), and a MALS photometer (DAWN HELEOS-II, Wyatt Technology Corp., 16 measurement angles, with nominal values ranging from 28° to 147°) followed by a DRI detector (T-rEX, Wyatt Technology Corp.). Normalization of the MALS detector (vacuum wavelength of incident light, $\lambda_0 = 664.5$ nm), inter-detector alignment, and inter-detector band broadening correction, the latter as described in Ref. [25], were performed using a low molar mass (15,000–20,000 g mol^{-1}) dextran sample from USB Corp. (Cleveland, OH). Due to the high concentration of this dextran sample solution ($c = 25$ mg mL^{-1}), the HF5 cartridge was replaced with a union in order to avoid unnecessary overloading of the fiber. The eluent was filtered online by placing a 0.22 μm inline nylon filter after the pump and before the injector.

The HF5 cartridge contained a 17 cm-long polyethersulfone (PES) fiber of 0.8 mm inner diameter, and 1.3 mm outer diameter, with a nominal cut-off of 10 kDa (Wyatt Technology Corp.). The HF5 analysis conditions are summarized in Table 1. For elution of polysaccharides, a linearly decaying cross flow starting from 0.2 mL min^{-1} was employed. All the analyses were carried out using H_2O + 0.02% NaN_3 as eluent. Detectors were temperature regulated at 25.0 ± 0.1 °C, while the HF5 fiber temperature was ambient. The polysaccharide samples were dissolved in eluent at concentrations between 0.5 mg mL^{-1} and 1 mg mL^{-1}, except for the lowest-*M* pullulan, which was analyzed at a concentration of 2 mg mL^{-1}.

The injection volume was 10 μL for all samples. Data collection and processing from HF5 analyses was performed using ASTRA

Table 1
HF5 analysis conditions for pullulans, dextrans, and larch arabinogalactan.[a]

Start time (min)	End time (min)	Mode	Cross flow F_x start (mL min^{-1})	Cross flow F_x end (mL min^{-1})	Focus flow (mL min^{-1})
0	2	Focus			0.65
2	5	Focus + Inject			0.65
5	25	Elution	0.2[b]	0.0[c]	
25	30	Elution + Inject	0.0	0.0	

[a] A constant channel flow of 0.5 mL min^{-1} was maintained throughout the analyses.
[b] Lower initial cross flow of 0.1 mL min^{-1} was used for dextran 1660000.
[c] Linear decay from 0.2 mL min^{-1} to 0.0 mL min^{-1} over 20 min.

software (v. 6.1.1.17, from Wyatt Technology Corp.). A first-order Zimm formalism was employed to fit the unsmoothed light scattering data.

2.3. ISIS peak simulations and size (R_H) calculations

In HF5, as in other FFF techniques, the translational diffusion coefficient D_T of an analyte can, in theory, be determined from the observed retention time t_R. The relationship between t_R and D_T is expressed by the following equation:

$$t_R = \frac{R^2}{8D_T} \ln \frac{F_{in}}{F_{out}} \quad (1)$$

where R is the internal radius of the hollow fiber, F_{in} is the flow rate entering the fiber, F_{out} is the flow rate at the fiber exit, and F_x is the rate of cross flow ($F_{out} = F_{in} - F_x$) [16]. The value of D_T obtained using Eq. (1) can then be used to calculate the hydrodynamic (Stokes) radius R_H of the analyte [3,26,27].

The application of Eq. (1) to isocratic FFF separations where, by definition, a constant cross flow is maintained, is a relatively straightforward task. In our experiments, however, the cross flow was not constant; rather, a linearly decaying cross flow gradient was employed, as given by the function $F_x(t) = -ta + F_x(0)$, where $F_x(t)$ is the cross flow at any given time t, $F_x(0)$ is the initial cross flow (i.e., at $t = 0$), and a is the slope of the gradient. One consequence of a linearly decaying cross flow gradient is that the ratio F_{in}/F_{out} is no longer constant during elution. In such case, accurate calculation of D_T (and, therefore, of R_H) necessitates accurate calculation of F_{in}/F_{out} at each time increment t.

The continuously changing boundary value problem described above lies within the purview of finite element methods and their implementation via finite element analysis [28]. Here, this has been done employing the Intelligent Separation Improvement System, ISIS (v. 1.2.0 (206)), from Superon GmbH. Using ISIS, calculation of t_R or R_H is made possible for time-dependent cross flows with either linearly or exponentially decreasing gradients. ISIS calculations also incorporate the temperature dependence of solvent or carrier liquid viscosity (needed for accurate calculation of R_H, as seen in the equation for R_H given at the bottom of Table 2), for experiments in either water or tetrahydrofuran (THF). All HF5 ISIS calculations or simulations require as input parameters the length and internal radius of the hollow fiber, as well as the identity of the solvent or carrier liquid employed, and the temperature at which the experiment is being conducted. For calculation of R_H distributions, ISIS employs an iterative method, the details of which can be found in Ref. 28, to originally calculate the distribution of D_T values from the experimentally determined t_R of an imported fractogram, along with the input parameters mentioned above and the profile of the separation gradient. Fractogram simulations are performed by providing the average size (R_H) of the eluting species. This type of simulation is particularly useful when attempting to determine whether a given set of experimental conditions (e.g., a particular combination of channel, cross, and focus flows) will allow for adequate separation of an analyte pair (in which case the sizes and respective mass fractions of the two components are required a priori), keeping in mind that, all other experimental factors being equal, the individual relationships among the retention times and hydrodynamic radii of two analytes will be proportional to one another. Intrafiber band broadening corrections are performed as described in Ref. [29]. It should be noted that both fractogram simulation and intrafiber band broadening correction in ISIS assume monodisperse species with Gaussian elution profiles, the latter as per the theory originally developed by Giddings et al. [30]. These assumptions can present a shortfall for cases such as polysaccharides, which are neither monodisperse nor, in many cases, do they possess Gaussian profiles. In Section 3.3 we take advantage of the power of ISIS to provide R_H distributions for the pullulans, dextrans, and arabinogalactan examined, and also explore the capabilities and limitations of the method with respect to the simulation of these polysaccharides' fractograms.

2.4. SEC analysis

A pullulan sample with nominal molar mass of 212,000 g mol^{-1} was analyzed by SEC/MALS/DRI in addition to HF5 to compare molar mass distributions and analysis recoveries from these different techniques. SEC analysis was conducted using the same instrumental set-up as for HF5 analysis, except without the Eclipse DualTec unit. Columns used for the SEC separation were a PL Aquagel-OH 40 and a PL Aquagel-OH 50 (Agilent/Polymer Laboratories, Amherst, MA) connected in series, with both of these columns having particle size of 15 μm. The flow-rate was 1 mL min^{-1} and injection volume 100 μL. Analysis was accomplished at 25 °C (temperature control for columns and detectors).

2.5. Off-line quasi-elastic light scattering (QELS) analysis

The R_H values for unfractionated pullulan, dextran, and arabinogalactan samples were determined by off-line QELS (Wyatt Technology Co.) at a nominal angle of 108°. Polysaccharide samples were dissolved in H_2O + 0.02% NaN_3 at a concentration of 15 mg mL^{-1} (dextran 50000), 5 mg mL^{-1} (pullulan 212000 and dextran 270000), or 3 mg mL^{-1} (pullulans 380000 and 1660000 and dextrans 670000 and 3500000), and filtered before analysis through 0.2 μm nylon syringe filters (Pall Corp., Ann Arbor, MI). Reliable QELS data could not be obtained for pullulan 22800, because it contained large-sized aggregates (as seen in the fractogram in Fig. 1a). Each sample was injected directly into the QELS photometer cell using a Razel model A-99EJ syringe pump at a flow rate of 0.1 mL min^{-1}. Correlation data from QELS were transformed into translational diffusion coefficients D_T using the method of cumulants [31] and thence to R_H via the well-known Stokes–Einstein equation (see equation at bottom of Table 2). Data were collected and processed with ASTRA software (Wyatt Technology Corp.) The measurements were performed at 25.0 ± 0.1 °C.

2.6. Specific refractive index increment ($\partial n/\partial c$) determination

The $\partial n/\partial c$ values for pullulan and dextran in H_2O + 0.02% NaN_3 at 25 °C were determined using pullulan with nominal

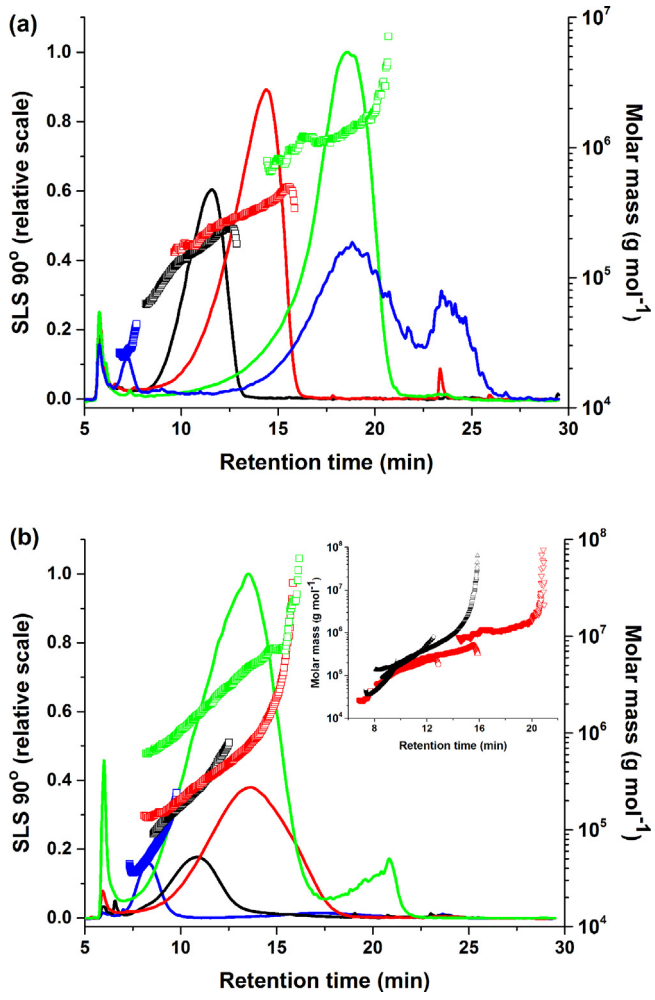

Fig. 1. Static light scattering signals (SLS 90°, solid lines) and molar masses (open squares) from HF5/MALS/DRI for (a) pullulans and (b) dextrans. In (a) blue trace corresponds to pullulan 22800, black to pullulan 212000, red to pullulan 380000, and green to pullulan 1660000, and in (b) blue corresponds to dextran 50000, black to dextran 270000, red to dextran 670000, and green to dextran 3500000. All the samples were analyzed using a similar HF5 method, except dextran 3500000, for which lower initial cross-flow was employed (see Table 1 for details of analysis conditions). (b, inset) Molar mass versus retention time for dextrans (black symbols) and pullulans (red symbols); dextran 3500000 is not included, as it was analyzed employing a different flow profile and, thus, its retention times are not comparable to those of the other polysaccharides plotted. (For interpretation of the references to color in this figure legend, the reader is referred to the web version of this article.)

M of 22,800 g mol^{-1} and dextran with nominal M of 15,000–20,000 g mol^{-1}. The dextran sample was dissolved in the solvent at concentrations ranging from 1 mg mL^{-1} to 6 mg mL^{-1}. For the pullulan sample, the concentrations ranged from 0.5 mg mL^{-1} to 5 mg mL^{-1}. Each dilution (six dilutions were employed for both pullulan and dextran) was injected directly into the DRI cell (same T-rEX detector as employed in the on-line experiments; vacuum wavelength of light $\lambda_0 = 658$ nm, within 7 nm of the λ_0 of the MALS photometer) the same way as in the off-line QELS analyses, using a Razel model A-99EJ syringe pump at flow rate of 0.1 mL min^{-1}, at 25.0 ± 0.1 °C. The samples were gently filtered before measurement through 0.2 μm nylon syringe filters (Pall Corp.). Data were collected using the ASTRA software. The $\partial n/\partial c$, obtained from the slope of a plot of concentration versus differential refractive index, was 0.135 ± 0.001 mL g^{-1} for dextran and 0.136 ± 0.001 mL g^{-1} for pullulan. Given the very small difference in $\partial n/\partial c$ values for dextran versus pullulan, also previously observed by others [34], a $\partial n/\partial c$ value of 0.135 mL g^{-1} was employed for arabinogalactan.

3. Results and discussion

3.1. HF5/MALS/DRI characterization of pullulans, dextrans, and larch arabinogalactan

In this study, HF5 coupled to both MALS and DRI detection was employed to characterize three structurally different polysaccharides: Pullulans, linear polysaccharides where (1→4)-α-D-linked maltotriose units are connected to each other via (1→6)-α-D-linkages; dextrans, (1→6)-α-D-linked glucans with branches at the (1→3)-α-D position; and larch arabinogalactan. The latter is a more structurally heterogeneous polysaccharide than are the previous two, being composed of a (1→3)-β-D-galactopyranosyl backbone with several different types of branching structures at position of C-6, mainly (1→6)-β-D galactopyranosyl monomers and dimers which, themselves, may also be further substituted at position of C-6 with β-L-arabinopyranosyl or α-L-arabinofuranosyl units. Additionally, larch arabinogalactan is known to contain single glucuronic acid units attached as side chains, a feature which, as we shall see in Section 3.2, appears to affect the recovery of these polysaccharides from the HF5 fiber [32,33]. To date, concentration-sensitive detection in HF5 has generally involved the use of UV spectroscopy, as the types of samples studied (proteins, polystyrene latexes) have possessed natural chromophores. As part of the present study, we also demonstrate how differential refractometry (DRI), a more universal concentration-sensitive

Table 2
Molar mass averages from HF5/MALS/DRI and z-average hydrodynamic radii ($R_{H,z}$) from off-line QELS of polysaccharides examined.

Sample[a]	M_w (g mol^{-1})	M_n (g mol^{-1})	Đ (vendor)	Đ (experimental)	$R_{H,z}$ [b] (nm)
Pullulan 22800	29,100 ± 300	28,200 ± 100	1.07	1.03 ± 0.01	nd[c]
Pullulan 212000	160,200 ± 8200	148,100 ± 4400	1.13	1.08 ± 0.06	13
Pullulan 380000	322,100 ± 13,300	301,200 ± 11,800	1.12	1.07 ± 0.06	16
Pullulan 1660000	1,229,000 ± 33,900	1,141,500 ± 38,900	1.19	1.08 ± 0.05	28
Dextran 50000	54,200 ± 1500	49,400 ± 200	1.36	1.10 ± 0.03	6
Dextran 270000	222,600 ± 100	182,700 ± 800	1.66	1.22 ± 0.01	11
Dextran 670000	521,900 ± 26,600	334,450 ± 5900	2.01	1.56 ± 0.08	18
Dextran 3500000	3,758,500 ± 170,400	1,840,000 ± 405,900	2.50	2.04 ± 0.46	30
Arabinogalactan	43,800 ± 1500	41,400 ± 800	na[d]	1.06 ± 0.04	3

$R_H \equiv k_B T/(6\pi\eta_0 D_T)$, where k_B is Boltzmann's constant, T is the absolute temperature, η_0 is the solvent viscosity at the experimental temperature, and D_T is the translational diffusion coefficient of the analyte. $Đ \equiv M_w/M_n$, where M_w is weight-average molar mass and M_n is number-average molar mass. Uncertainties in molar mass averages and dispersity represent 1 standard deviation based on duplicate injections.

[a] Numbers after polysaccharide names represent the nominal molar masses, in g mol^{-1}, provided by the vendors.
[b] From off-line QELS (see Section 2.4 for details). In all cases, instrumental standard deviations <±1 nm.
[c] Aggregation in solution precluded reliable determination of R_H for this sample. See text for details.
[d] Dispersity data for this polysaccharide not available from manufacturer.

detection method than UV, can be used in conjunction with HF5/MALS.

Fig. 1a overlays the fractograms of pullulans with varying molar masses and Fig. 1b is the corresponding overlay for dextrans; an overlay of molar mass versus retention time for both sets of polysaccharides is shown in the inset to Fig. 1b. Both pullulans and dextrans elute according to normal mode FFF theory, as smaller-sized analytes (which, for linear macromolecules, corresponds to smaller M analytes) elute before larger ones. Because of their branched structure, dextrans are known to possess a more compact solution conformation than do pullulans, which are linear, of the same M [34]. The consequence of this can be observed in Fig. 1b, inset, where, at a given retention time, the M of the dextrans is larger than that of the pullulans (except at the lowest M, where branching in dextrans is known to be both sparse and short-chained) or, conversely, where for a given M the retention time of the branched dextrans is seen to be smaller than that of the linear pullulans. While the molar masses obtained here for most polysaccharides are somewhat lower than the nominal values provided by the manufacturer (Table 2), the experimentally obtained and manufacturer-provided values are found to be comparable to each other, as are the respective molar mass dispersities (defined as the ratio M_w/M_n of each polysaccharide). The difference in M dispersities between dextrans and pullulans is reflected in the breadth of their HF5 peaks in Fig. 1, with the peaks of the larger-dispersity dextrans being broader than those of the lower-dispersity pullulans. With the experimental conditions employed (Table 1), characterization of polysaccharides with M ranging from ≈23,000 g mol^{-1} to ≈7,500,000 g mol^{-1} could be obtained within 25 min employing HF5/MALS/DRI. Similar conditions were used for all samples except for the highest-M dextran (dextran 3500000), for which a lower initial cross-flow was employed to decrease the peak width of this highly disperse sample. Due to this difference in cross-flow between dextran 3500000 and the other dextrans and pullulans examined, the retention time of dextran 3500000 (green trace in Fig. 1b) cannot be compared directly with the retention times of other polysaccharides examined and, consequently, M data for this polysaccharide are not included in the inset in Fig. 1b.

An interesting case occurs for the molar mass of the lowest-M pullulan examined, pullulan 22800, where the M_w determined by HF5/MALS/DRI was ≈20% higher than the nominal value provided by the manufacturer (Table 1 and Fig. 1a). This difference in molar masses is likely a consequence of the smallest-sized, lowest M part of the sample having been lost by permeation through (or irreversible sorption onto) the porous fiber walls, meaning that only the higher M portion of the sample eluted from the fiber into the detectors, thus biasing the calculated M averages to artificially high values. This sample loss is confirmed by the low sample recovery for this pullulan based on the peak area measured by the DRI detector and the $\partial n/\partial c$ value obtained by off-line DRI analysis (see Section 3.2 for a discussion of analysis recovery and Section 2.5 for $\partial n/\partial c$ determination). In fact, the molecular size of pullulan 22800 was found to be very close to the pore size of the fiber. According to calculations based on the observed HF5 retention times, the R_H of this lowest-M pullulan is only ≈3 nm, whereas the nominal cut-off of the fiber is 10 kDa, which has been reported to correspond to an average pore diameter of 5 nm [20]. The other feature that distinguishes pullulan 22800 from the other pullulans analyzed is the large, bimodal broad peak that elutes during the latter half of the cross-flow gradient (between 12 min and 27 min; note that all times given in the manuscript and in the figures are retention times, not elution times, i.e., they denote the time transpired since the beginning of the experiment, *not* since elution of the void peak), which can be clearly seen in the 90° static light scattering (SLS) fractogram of this polysaccharide in Fig. 1a. This peak likely originates from large-sized aggregates which, even though they appear

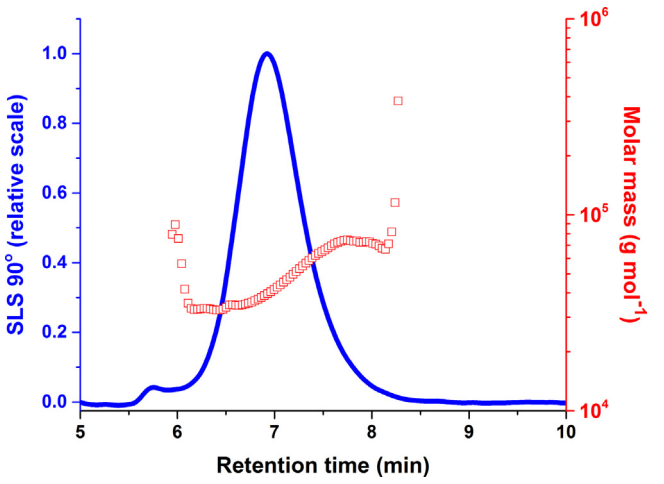

Fig. 2. Static light scattering signals (SLS at 90°, solid blue line) and molar mass (open red squares) from HF5/MALS/DRI for larch arabinogalactan. (For interpretation of the references to color in this figure legend, the reader is referred to the web version of this article.)

to mostly be separated by HF5 from the main, non-aggregated pullulan, may also provide some minor contribution to the elevated (as compared to the nominal) M values found for this polysaccharide. The presence of aggregates (which, also using MALS, have previously been observed for other pullulans when dissolved in complex polar aprotic solvents) [35] was also deduced here from the off-line QELS analysis of pullulan 22800. Because off-line QELS provides the average size of the bulk, unseparated sample, and because the sample solution contained both individual polysaccharide chains as well as aggregates, an unrealistically high R_H value (≈38 nm, not given in Table 2 so as to avoid confusion) was obtained from off-line QELS. The fact that aggregates were also present in the off-line QELS experiments is evidence that aggregation is an intrinsic property of this particular sample solution and not an artifact arising from the HF5 analysis (e.g., aggregate formation during the focusing and/or elution step). What structural and/or chemical features are responsible for the aggregation of this particular pullulan at the given solvent/temperature conditions, while the other pullulans do not appear to exhibit measurable aggregation at the same conditions, remains an open question at this time, however.

Besides dextran, arabinogalactan from larch wood represents another example of a branched polysaccharide, though, as mentioned earlier, one with a more complex structure. Arabinogalactan from larch wood has been found to consist of two populations that differ in their molar masses: A less abundant, less branched lower-molar mass component and a more abundant, more highly branched higher-molar mass component [36]. The average molar masses reported for these two fractions vary in the literature. According to ultracentrifugation experiments that were performed 65 years ago, the M_w of lower-molar mass fraction is 16,000 g mol^{-1} and that of the higher-M fraction 100,000 g mol^{-1} [37]. While previous studies, employing SEC with a universal calibration approach, agreed with these findings (the predominant population was found to have $M_w \approx 90{,}000$ g mol^{-1} and the less abundant fraction to have $M_w \approx 14{,}000$ g mol^{-1}) [38], other SEC studies indicated significantly lower M values for both fractions [36,39]. These latter SEC experiments suggest an $M_w \approx 7500$ g mol^{-1} for the lower-molar mass fraction and ≈40,000 g mol^{-1} for the higher-molar mass fraction. It is important to note here that great variability can be exhibited in the chain lengths of plant polymers depending on factors such as their source, environmental stresses, age, genotypes, etc.

As can be observed in Fig. 2, HF5 is able to distinguish the two populations present in Type II larch arabinogalactan, as well as their abundance relative to each other. The first eluting peak, eluting between 5.5 min and 6 min, represents the lower-molar mass fraction of the sample. It should be remembered that in HF5 smaller analytes elute ahead of larger ones, similar to the case in AF4 and opposite that in SEC or HDC. It is likely that a portion of this low-*M* fraction has permeated through the HF5 fiber wall, however, lowering the intensity of the MALS and DRI peaks and thus precluding determination of the molar mass of this portion of the analyte. In addition, the HF5 void peak also elutes at a retention time of 5.8 min. However, the S/N of the void peak in a solvent blank is ≈2, while in fractograms of arabinogalactan the S/N of the 5.8 min peak is 7 (in both cases based on the signal from the 90° MALS photodiode), confirming that in the arabinogalactan fractograms this peak does, indeed, belong predominantly to the low-*M* fraction of the sample. For the high-*M* fraction (eluting between 6 min and 8.5 min), the molar mass across the fractogram ranges from 33,000 g mol^{-1} to 74,000 g mol^{-1}, as shown in Fig. 2. This molar mass range is consistent with that obtained previously by SEC [36,39].

The most significant challenge in coupling both MALS and DRI detection to HF5 is the relatively low fiber volume, which restricts sample load. Thus, the S/N ratio of these detectors might be too low for molar mass and size determination. Conversely, a low fiber volume is advantageous when a limited amount of analyte is available. The volume of the fiber used in this study was 85 μL and amounts injected varied between 5 μg and 20 μg. With these amounts a sufficient S/N ratio for both MALS and DRI detectors was obtained, which allowed determination of the molar mass of all polysaccharides across the fractogram of each (Figs. 1 and 2). It is noteworthy to mention that recoveries from HF5 were not 100% (analysis recovery is discussed in more detail in the next section), indicating that even lower amounts might have sufficed for accurate molar mass determination. However, even for the highest-*M* samples, the MALS S/N was too low to allow for accurate determination of the radius of gyration, R_G (while the smallest samples did not possess sufficient angular dissymmetry for measurement of R_G at the given solvent/temperature/wavelength conditions). It should also be noted that the branched nature of both dextran and arabinogalactan is expected to generate local architectural polydispersity in the fractograms (i.e., architecturally different structures may co-elute due to a coincidence in their D_T) [14], not accounted for here in the *M* versus retention time relationships due to the just-mentioned inability to measure size on-line, across the fractograms.

3.2. Sample recovery from HF5

Analysis recoveries from HF5 were calculated from the on-line DRI signals, using the measured $\partial n/\partial c$ values for pullulan and dextran (see Section 2.5). As mentioned in Section 2, given that the $\partial n/\partial c$ values for these two polysaccharides differed from each other by only 1 part per thousand, and that the $\partial n/\partial c$ values of most polysaccharides have been found to be similar to one another at the same experimental conditions, the same value as for dextran was employed for the arabinogalactan sample examined.

The recoveries from fractionation exceeded 70% for all the dextran samples. However, sample recovery for the pullulans was lower, less than 50%. In principle, four reasons could lead to low analyte recoveries in HF5 (as well as in other flow FFF techniques). The first reason for low analyte recovery could be insufficient focusing of the analytes. If the HF5 focusing time is too short and/or the focusing flow rate too low, part of the sample may co-elute with the void peak. The intensities of the void peaks observed in the pullulan fractograms in Fig. 1a (at a retention time of 5.8 min) are, nevertheless, comparable with the ones in the dextran fractograms (Fig. 1b), indicating a similar focusing effect in the case of both the pullulan and dextran samples (i.e., in both cases the focusing procedure was able to resolve the analyte peak from the void peak). Second, analyte molecules may interact reversibly with the fiber wall as a consequence of the radial transport forces generated by the cross flow (and/or by the focus flow). In this case, the retained molecules elute after switching the cross flow off. In the pullulan fractograms, however, no peaks were observed after the cross flow decreased to 0 mL min^{-1} (retention times >25 min). Thus, this explanation does not seem likely, either. The third reason for low recoveries is irreversible adsorption of analyte molecules to the fiber walls. That might explain, at least partly, the low recoveries of pullulans, as could the fourth and the final reason, transport of analyte molecules through the porous fiber walls during analysis. That this last is an actual concern is demonstrated by the analysis of two oligosaccharides, maltoheptaose and isomaltoheptaose, with the latter being an oligomer of pullulan (see Supplementary Information for further details). (It should be noted that incomplete sample solubility may give the appearance of low analyte recovery in any chromatographic or FFF analysis. However, the fact that pullulans are highly water-soluble, combined with the results from the SEC experiments with pullulan 212000, allow us to rule out this scenario).

To exclude the effect of separation conditions on pullulan recovery values in HF5, an initial cross-flow of 0.1 mL min^{-1} and a focus flow of 0.2 mL min^{-1} were employed to analyze pullulan 212000, instead of the respective 0.2 mL min^{-1} and 0.65 mL min^{-1} flows (these flows were changed one at a time; otherwise, flow conditions correspond to the ones presented in Table 1). The fractograms and recovery values from the analyses are shown in Fig. S2. This pullulan sample eluted earlier when using an initial cross flow of 0.1 mL min^{-1} (green line in Fig. S2) instead of 0.2 mL min^{-1} (black line in Fig. S2), as expected. The recovery values were, however, essentially identical to each other, 50% versus 49%. Thus, cross flow does not appear to have a significant effect on pullulan recovery in these experiments. Using a lower focus flow of 0.2 mL min^{-1} (red line in Fig. 4) instead of 0.65 mL min^{-1} seemed to lower sample recovery even more, from 49% to 30%. We thus conclude that lowering either the cross-flow or the focus flow does not increase pullulan recovery in HF5 under the present solvent/temperature conditions.

When the analysis of a homopolymer displays low sample recovery, as is the case here with the HF5 analysis of pullulan, it is extremely important to determine whether the portion of the sample that was actually detected and characterized is biased with respect of molar mass (or size). Because HF5 recovery values for pullulans were ≤50%, regardless of the flow conditions employed, we analyzed pullulan 212000 by SEC/MALS/DRI at the same solvent/temperature conditions as in HF5 (see Section 2.4 for SEC experimental details), to compare the molar mass distributions obtained for this polysaccharide employing the two different separation techniques. The overlay of the MMDs obtained by HF5 and by SEC is presented in Fig. 3. As can be seen, the distributions are very similar to each other. This consistency indicates that the portion of the sample that was detected in HF5 appears to be unbiased with respect to molar mass. Furthermore, the recovery from the SEC analysis was high (98%, which, as mentioned earlier, provides strong evidence that low sample solubility is not responsible for the low analysis recovery); thus, the distribution obtained by SEC can be considered to well represent the sample as a whole and to support the argument that the same is true in the HF5 analysis of pullulans at the given experimental conditions. A similar consistency among molar mass results obtained by AF4 and SEC, when recoveries were significantly lower in the former technique as compared to the latter, was previously observed for guar galactomannan [40].

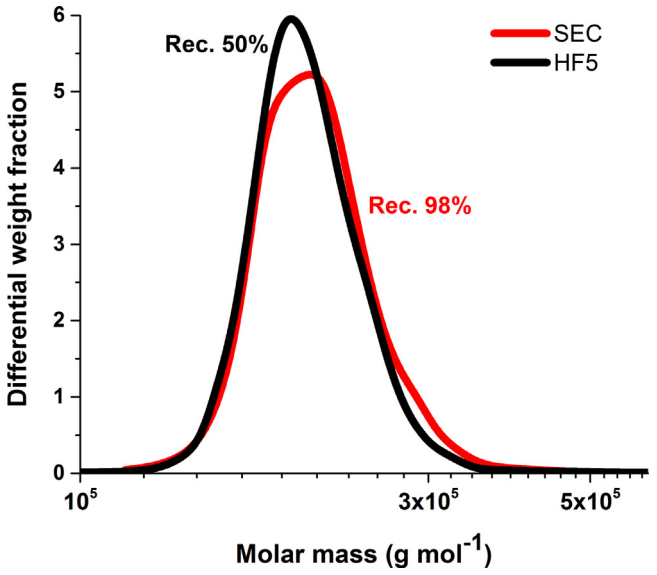

Fig. 3. Overlay of differential molar mass distributions for pullulan 212000 obtained by HF5 (black line) and SEC (red line). The initial cross-flow for HF5 analysis was 0.1 mL min^{-1}. Despite a significance difference in analysis recovery values ("Rec."), the similarity of the MMDs indicates that, in HF5, the analyzed portion of the pullulans is representative of the total molar mass population of the polysaccharides. (For interpretation of the references to color in this figure legend, the reader is referred to the web version of this article.)

Arabinogalactan sample recovery from HF5 was 61%. This value can be regarded as surprisingly high, given the relatively low molar mass of the arabinogalactan sample examined and the fact that its size (as given by R_H) is almost identical to that of pullulan 22800 (≈3 nm), for which HF5 recovery was extremely low (<10%). We believe the main reason behind the higher (as compared to pullulan) arabinogalactan recovery is that this polysaccharide contains glucuronic acid side units (1% of total monosaccharide constituents) [33]. The negative charges caused by dissociated acidic side groups can induce repulsive forces with the negatively charged polyethersulfone fiber, preventing arabinogalactan molecules from reaching close proximity to the fiber surface and, thus, from permeating through the fiber walls.

3.3. R_H distribution calculation and comparison to off-line QELS; fractogram simulation

As described in Section 2.3, the ISIS software was employed to implement HF5 theory for the calculation of D_T and, hence, of R_H, in the case of a linearly decaying cross flow gradient such as that employed in the present study. This type of transformation allowed the fractograms of the polysaccharides to be converted into R_H distributions, shown in Fig. 4 for both the pullulans and dextrans examined. As already discussed, the lowest-M pullulan (pullulan 22800) aggregated in solution; its broad peak (10–60 nm) in Fig. 4a (blue line) originates from these large-sized aggregates. All the samples were also analyzed by off-line QELS, which provided experimentally obtained $R_{H,z}$ values (Table 2) to which the R_H values obtained from HF5 could be compared. We note that the R_H obtained by off-line QELS agree well with previously published R_H values (obtained at similar solvent/temperature conditions) for both pullulans and dextrans, providing confidence in the accuracy of the present measurements [34,41].

The R_H values determined by off-line QELS all fall well within the range of the calculated R_H distributions. However, most of the experimental values are located in the middle or lower end of the distribution. This is a counterintuitive finding, given that

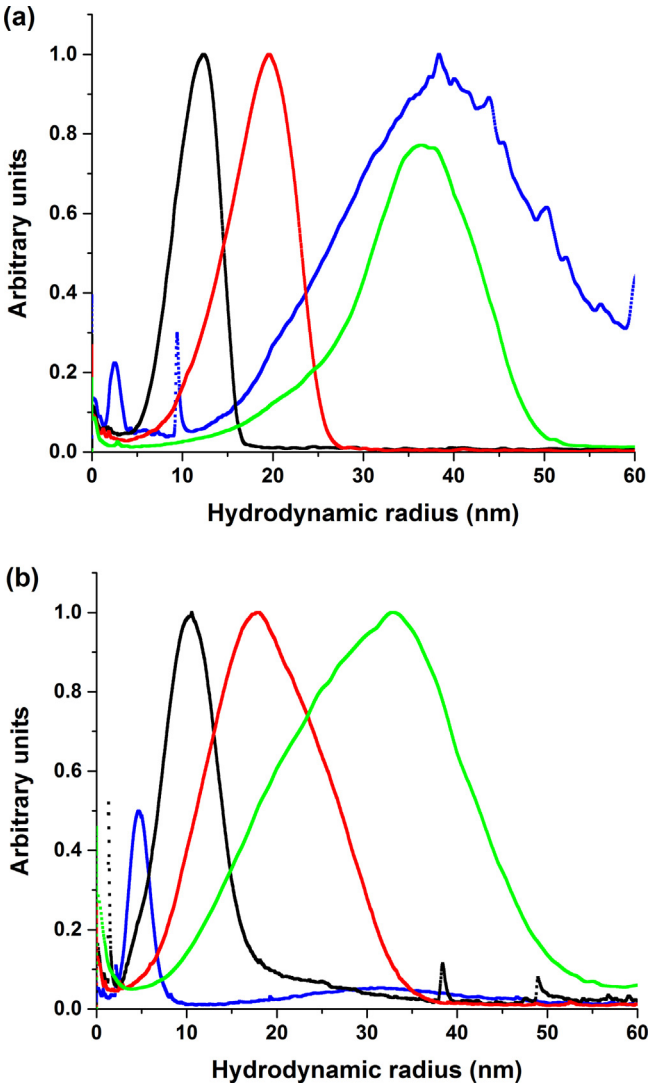

Fig. 4. Calculated R_H distribution, based on applying FFF theory to HF5/MALS (90° signal) fractograms, for (a) pullulans and (b) dextrans. In (a) blue trace corresponds to pullulan 22800, black to pullulan 212000, red to pullulan 380000, and green to pullulan 1660000 and in (b), blue corresponds to dextran 50000, black to dextran 270000, red to dextran 670000, and green to dextran 3500000 (same color coding as in Fig. 1). (For interpretation of the references to color in this figure legend, the reader is referred to the web version of this article.)

the experimental values are z-averages, a statistical moment that is representative of the higher (large-sized) end of the distribution. We attempt to explain this discrepancy as follows. If we assume the off-line QELS values to be closer to "true" R_H values (an assumption which is bolstered by their agreement with previous, independently determined literature data, as noted above), then the R_H values from HF5 are being overestimated. In other words, the retention times of the samples are larger than expected. Similar observations have been reported for pullulans in AF4 analysis [42,43]. In said studies, both constant and exponentially decaying cross flow conditions were employed: The R_H values of those pullulans were determined by AF4 under isocratic conditions and these values were then used for calculation of expected retention times in AF4 analyses employing an exponentially decaying cross-flow gradient. The researchers found that, for pullulans with $M > 400{,}000$ g mol^{-1}, the observed retention times in the gradient analyses were higher than the retention times predicted from the hydrodynamic sizes of the polysaccharides. This late elution was explained by a secondary relaxation effect which is known to occur

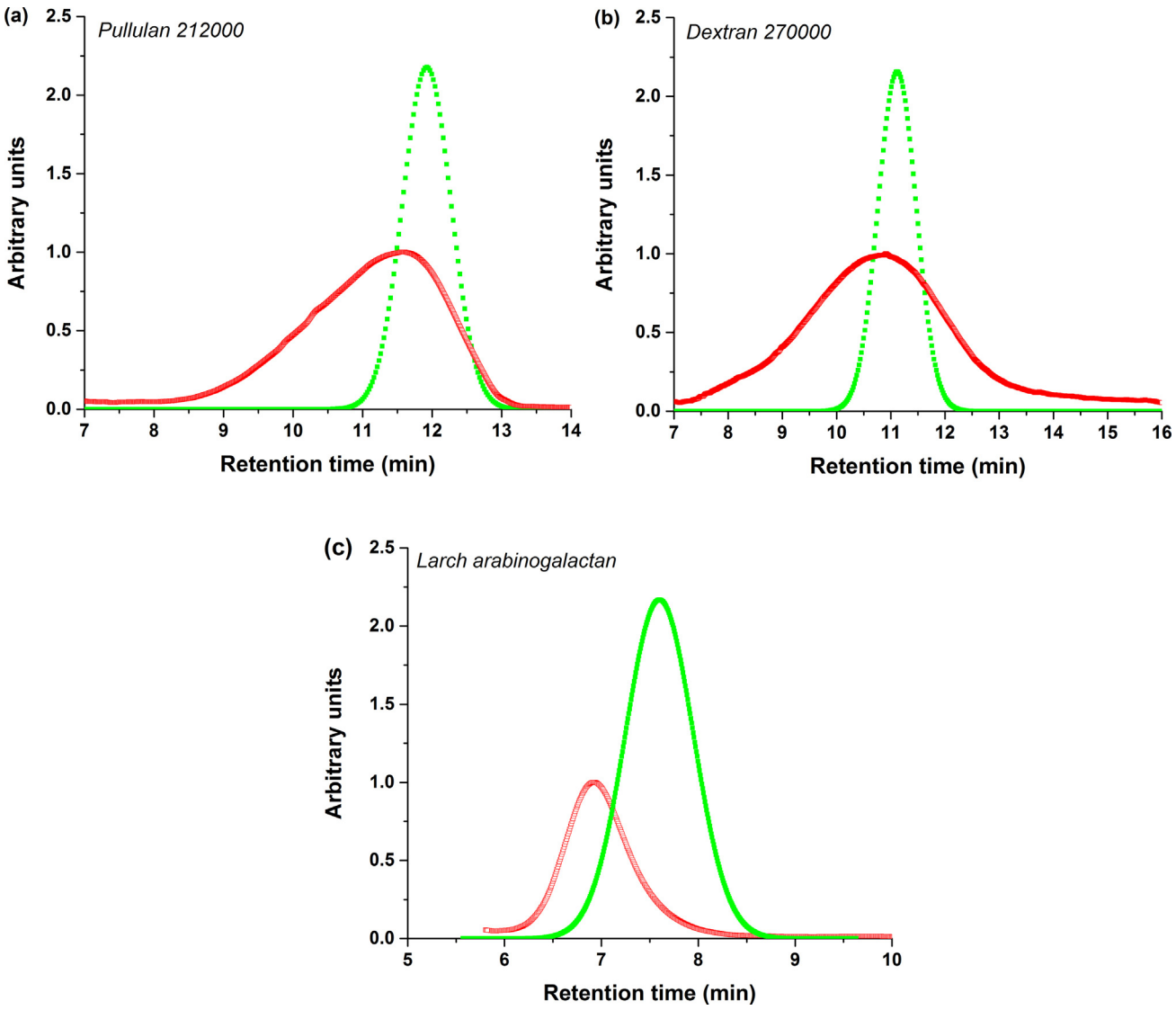

Fig. 5. Experimentally determined versus simulated HF5 fractograms of (a) pullulan 212000, (b) dextran 270000, and (c) larch arabinogalactan (higher-*M* fraction, see text for details). In all cases, red open squares represent experimental fractograms (90° SLS) obtained using flow conditions summarized in Table 1, green solid squares represent the simulated fractograms based on the R_H obtained from off-line QELS and the input parameters detailed in Section 2.3. (For interpretation of the references to color in this figure legend, the reader is referred to the web version of this article.)

in field-flow fractionation when cross-flow gradients are employed [44]: When field strength (cross flow) changes as a function of time, the sample molecule cloud moving in the parabolic flow profile may lag behind in a steady state configuration (i.e., not moving away from the accumulation wall/fiber wall as expected as cross-flow decreases). This lag results in higher retention times, lower apparent D_T values and, hence, larger calculated values of R_H. Because larger molecules need more time to achieve a steady state in the AF4 channel or HF5 fiber than do smaller molecules, these secondary relaxation effects are more pronounced for the larger molecules. It is also possible that the late elution of the, especially, high molar mass molecules is caused by their immobilization at the channel/fiber wall until the cross-flow is significantly decreased [43]. Both these factors, secondary relaxation effects and immobilization at the hollow fiber wall, may have caused slightly higher retention times for the highest-*M* pullulans and dextrans in our HF5 analyses, resulting in the reported discrepancy in the location on the calculated R_H distribution of the experimentally determined $R_{H,z}$ averages.

One additional reason for the above-mentioned discrepancy between the experimentally determined $R_{H,z}$ values and their location in the calculated R_H distributions results from the very definition of R_H which can be written as [26]:

$$R_H \equiv \left(\frac{1}{n} \sum_{n=1}^{n} \left\langle \frac{1}{r_n} \right\rangle_z \right)^{-1} \quad (2)$$

where the brackets ⟨⟩ represent the average of all possible reciprocal distances $1/r_n$, further averaged over all possible conformations; the index n represent the number of monomer units between two segment points in the polymer; and the index z indicates that the z-average of the MMD need be accounted for. This means that R_H is actually the z-average of the distribution of the first moment of sizes. However, R_H distributions from HF5 (Fig. 4) are not based on concentration fractograms from the DRI (due to low S/N in this detector's response) but, rather, on MALS fractograms (from the 90° MALS photodiode). Because LS response is directly proportional to M, larger M give rise to larger LS signals. An R_H distribution derived via FFF theory and using an LS-obtained fractogram will not correspond to a distribution of the first moment of sizes, as it would if a DRI obtained fractogram had been employed for this purpose; rather, the distribution will be artificially skewed toward higher R_H

values. This "effect" would further exacerbate those mentioned in the previous paragraph as possibly being responsible for the relatively low location of the experimentally determined R_H values on the calculated R_H distribution.

The ISIS software can also be employed to simulate HF5 fractograms. As described in Section 2.3, input parameters include analyte R_H, fiber dimensions, solvent, temperature, and flow profile. The flow profiles described in Table 1 were employed, in conjunction with the $R_{H,z}$ values obtained by off-line QELS and given in Table 2, to simulate fractograms of the various polysaccharides. Representative examples of the simulated fractograms, upon which are overlaid the experimentally determined data, are shown in Fig. 5a–c, for pullulan 212000, dextran 270000, and larch arabinogalactan, respectively. An examination of these overlays is instructive.

First, the simulated fractograms of pullulan 212000 and dextran 270000 are substantially narrower than are the experimentally determined fractograms of these polysaccharides, while the breadths of the simulated and experimental fractograms of arabinogalactan are nearly identical. The reason behind these observations lies in the assumption employed by the ISIS software of a perfectly monodisperse analyte, the fractographic breadth of which will then be due only to van Deemter-type band broadening processes during the separation. The dextran and pullulan samples in Fig. 5 are far from monodisperse, however, the M range of the former spanning from approximately 8×10^4 g mol^{-1} to 8×10^5 g mol^{-1} and that of the latter from approximately 6×10^4 g mol^{-1} to 2.5×10^5 g mol^{-1} (Fig. 1a and b). The software also employs the original assumption of Giddings et al. of Gaussian peaks [30] which, as can be seen in the case of pullulan 212000, does not always resemble reality in the world of natural polymers. Regardless, in both cases the apex of the experimentally determined peak lies within the simulated fractogram (for reasons analogous to why the respective R_H values determined by off-line QELS fall within the calculated R_H distributions, as discussed above) and the retention times of the peak apexes of the experimental fractograms are nearly coincident with the retention times predicted by the simulations for both pullulan 212000 and dextran 270000.

In the case of arabinogalactan, the experimentally determined and simulated peak breadths are quite similar to one another. This similarity is a reflection of the narrower M (and, consequently, size) dispersity in arabinogalactan, the M range of which spans from approximately 3×10^4 g mol^{-1} to 7.5×10^4 g mol^{-1} (Fig. 2), as compared to pullulan 212000 and dextran 270000; i.e., arabinogalactan more closely resembles the monodisperse assumption of the ISIS software than do either the pullulan or the dextran. The near-Gaussian shape of the peak of the main component of larch arabinogalactan also means that the peak shape of this polysaccharide is adequately represented by ISIS. Experimentally, however, the arabinogalactan is observed to elute from the hollow fiber earlier than predicted by the simulation; there is a large discrepancy between the retention times of peak apexes of the experimental and simulated fractograms, so much so that the apex of the experimental fractogram only barely overlaps the simulated peak. We attempt to explain this discrepancy as follows.

When the HF5 fractogram of larch arabinogalactan was converted into an R_H distribution (not shown), the R_H peak apex corresponded to a value of ≈2 nm. This value is slightly lower than the one obtained from off-line QELS (≈3 nm). Thus, if we assume the QELS value to be accurate, arabinogalactan elutes in HF5 slightly earlier than expected (Fig. 5c). This scenario is highly probable due to the charged nature of the sample. As discussed already in Section 3.2, larch arabinogalactan contains glucuronic acid side groups. When dissociated in water, these groups carry a negative charge which can induce repulsive forces with the negatively charged PES fiber wall. As a result of this repulsive interaction between the arabinogalactan and the walls of the hollow fiber, the sample molecules move farther away from the fiber wall than expected, placing the molecules in faster streamlines than expected based on ideal, neutral analyte behavior which, in turn, results in earlier elution than predicted by FFF theory.

4. Conclusions

We have demonstrated here the applicabilty of commercial HF5 instrumentation to the analysis of polysaccharides, with the HF5 cartridge connected on-line to both MALS and DRI detection for the analysis of dextrans, pullulans, and larch arabinogalactan. The detectors employed allowed the determination of molar mass across the peaks of the fractograms, even though the amount of polysaccharide injected onto the hollow fiber was relatively low. The HF5/MALS/DRI analyses were complemented by off-line QELS determination of the z-average hydrodynamic radius $R_{H,z}$, and by calculations of the R_H distribution and by simulation of fractograms, the latter two based on a finite element analysis implementation of FFF theory by commercial software. In general, good agreement was obtained between the off-line QELS determined R_H of the dextran and pullulans and the values of this same radius as calculated from theory. Sample recovery from the HF5 system was determined in all cases and found to be higher for the dextrans than for the pullulans. Comparison between HF5/MALS/DRI and SEC/MALS/DRI analysis of the latter polysaccharides showed that analyte loss in HF5 of pullulans is unbiased, however, meaning that the technique provides a representative analysis of the molar mass of these polysaccharides under the present experimental conditions.

We hope that the experiments outlined here serve to introduce HF5/MALS/DRI for the purposes of polysaccharide characterization and the suitability of DRI as a concentration-sensitive detector for the analyses. To assess the accuracy of the method, we have concentrated on the analysis of well-characterized polysaccharides. The ultimate power of the technique, however, will lie in its ability to characterize ultra-high-M polysaccharides that are not amenable to either SEC or HDC analysis, and/or in cases where a higher sensitivity or a lower propensity for channel overloading and analyte aggregation is needed than generally provided by AF4. These advantages are augmented by the ease of installation, manufacturing reliability, and disposable nature of commercially available HF5 cartridges, and by the possibility of augmenting HF5 analysis with in silico simulations and off-line analyses.

Acknowledgements

The Finnish Cultural Foundation is acknowledged for financial support of L.P. through the Foundations' Post Doc Pool. The authors would also like to thank Päivi Tuomainen and Maija Tenkanen from the University of Helsinki for providing dextran samples, and Christoph Johann from Wyatt Europe and Superon GmbH for assistance with the ISIS software. Commercial products are identified to specify adequately the experimental procedure. Such identification does not imply endorsement or recommendation by the National Institute of Standards and Technology, nor does it imply that the materials identified are necessarily the best available for the purpose.

Appendix A. Supplementary data

Supplementary data associated with this article can be found, in the online version, at http://dx.doi.org/10.1016/j.chroma.2014.12.070.

References

[1] A.M. Striegel, Separation science of macromolecules: what is the role of multidetector size-exclusion chromatography? in: A.M. Striegel (Ed.), Multiple Detection in Size-exclusion Chromatography, American Chemical Society, Washington, DC, 2005, pp. 2–12.
[2] A.M. Striegel, W.W. Yau, J.J. Kirkland, D.D. Bly, Modern Size-exclusion Liquid Chromatography, John Wiley & Sons, New Jersey, 2009.
[3] A.M. Striegel, Multiple detection in size-exclusion chromatography of macromolecules Anal. Chem. 77 (2005) 104A–113A.
[4] R.L. Whistler, J.N. BeMiller (Eds.), Industrial Gums, third ed., Academic Press, San Diego, 1993.
[5] H.G. Barth, F.J. Carlin Jr., A review of polymer shear degradation in size-exclusion chromatography, J. Liq. Chromatogr. 7 (1984) 1717–1738.
[6] A.M. Striegel, Observations regarding on-column, flow-induced degradation during SEC analysis, J. Liq. Chromatogr. Relat. Technol. 31 (2008) 3105–3114.
[7] A.M. Striegel, Do column frits contribute to the on-column, flow-induced degradation of macromolecules? J. Chromatogr. A 1359 (2014) 147–155.
[8] A.M. Striegel, S.L. Isenberg, G.L. Cote, An SEC/MALS study of alternan degradation during size-exclusion chromatographic analysis, Anal. Bioanal. Chem. 394 (2009) 1887–1893.
[9] R.A. Cave, S.A. Seabrook, M.J. Gidley, R.G. Gilbert, Characterization of starch by size-exclusion chromatography: the limitations imposed by shear scission, Biomacromolecules 10 (2009) 2245–2253.
[10] A.M. Striegel, A.K. Brewer, Hydrodynamic chromatography, Annu. Rev. Anal. Chem. 5 (2012) 15–34.
[11] A.M. Striegel, Hydrodynamic chromatography: packed columns, multiple detectors, and microcapillaries, Anal. Bioanal. Chem. 402 (2012) 77–81.
[12] S. Podzimek, Light Scattering. Size Exclusion Chromatography and Asymmetric Flow Field Flow Fractionation, Wiley, New York, 2011.
[13] S.L. Isenberg, A.K. Brewer, G.L. Cote, A.M. Striegel, Hydrodynamic versus size exclusion chromatography characterization of alternan and comparison to off-line MALS, Biomacromolecules 11 (2010) 2505–2511.
[14] (a) R.G. Gilbert, Size-separation characterization of starch and glycogen for biosynthesis-structure-property relationships, Anal. Bioanal. Chem. 399 (2011) 1425–1438;
(b) M.J. Gidley, I. Hanashiro, N.M. Hani, S.E. Hill, A. Huber, J.L. Jane, Q. Liu, G.A. Morris, A. Rolland-Sabaté, A.M. Striegel, R.G. Gilbert, Reliable measurements of the size distributions of starch molecules in solution: current dilemmas and recommendations, Carbohydr. Polym. 79 (2010) 255–261.
[15] H.L. Lee, J.F.G. Reis, J. Dohner, E.N. Lightfoot, Single-phase chromatography. Solute retardation by ultrafiltration and electrophoresis, AIChE J. 20 (1974) 776–784.
[16] J.A. Jönsson, A. Carlshaf, Flow field flow fractionation in hollow cylindrical fibers, Anal. Chem. 61 (1989) 11–18.
[17] J.E.G.J. Wijnhoven, J.P. Koorn, H. Poppe, W.T. Kok, Hollow-fiber flow field-flow fractionation of polystyrene sulfonates, J. Chromatogr. A 699 (1995) 119–129.
[18] W.J. Lee, B. Min, M.H. Moon, Improvement in particle separation by hollow fiber flow field-flow fractionation and the potential use in obtaining particle size distribution, Anal. Chem. 71 (1999) 3446–3452.
[19] A. Zattoni, S. Casolari, D.C. Rambaldi, P. Reschiglian, Hollow-fiber flow field-flow fractionation, Curr. Anal. Chem. 3 (2007) 310–323.
[20] C. Johann, S. Elsenberg, U. Roesch, D.C. Rambaldi, A. Zattoni, P. Reschiglian, A novel approach to improve operation and performance in flow field-flow fractionation, J. Chromatogr. A 1218 (2011) 4126–4131.
[21] J.E.G.J. Wijnhoven, J. Koorn, H. Poppe, W.T. Kok, Influence of injected mass and ionic strength on retention of water-soluble polymers and proteins in hollow-fiber flow field-flow fractionation, J. Chromatogr. A 732 (1996) 307–315.
[22] H. Susanto, S. Franzka, M. Ulbricht, Dextran fouling of polyethersulfone ultrafiltration membranes-causes, extent and consequences, J. Membr. Sci. 296 (2007) 147–155.
[23] S. Elsenberg, T. Jocks, C. Johann, Hollow fibre flow field flow fractionation (HF5) increases sensitivity and efficiency in the separation of proteins and complex protein mixtures, Chromatogr. Today 5 (2012) 59–62.
[24] U. Rösch, W. Jevdokimov, German patent 10 2010 043 877 B3 (2012); U.S. Patent 2012/0119491 A1 (2012).
[25] S. Trainoff, U.S. Patent 7,386,427 (2008).
[26] W. Burchard, Solution properties of branched macromolecules, Adv. Polym. Sci. 143 (1999) 113–194.
[27] M.J. Smith, I.A. Haidar, A.M. Striegel, Measuring the size of polymers with negative radii using MALS/QELS: an exploration of the thermodynamic radius, Analyst 132 (2007) 455–460.
[28] (a) G. Strang, G. Fix, An Analysis of the Finite Element Method, Prentice Hall, Upper Saddle River, NJ, 1973;
(b) R.E. White, Introduction to the Finite Element Method with Applications to Nonlinear Problems, Wiley, New York, 1985;
(c) M. Mori, The Finite Element Method and Its Applications, McMillan, New York, 1983;
(d) J.N. Reddy, An Introduction to the Finite Element Method, McGraw-Hill, New York, 1984;
(e) H.R. Schwartz, Finite Element Methods, Academic Press, London, 1988.
[29] C. Johann, A. Kaltenborn, H. Schuch, M. Schumacher, European Patent EP2104853 B1 (2010).
[30] J.C. Giddings, Y.H. Yoon, K.D. Caldwell, M.M. Myers, M.E. Hovingh, Nonequilibrium plate height for field-flow fractionation in ideal parallel plate columns, Sep. Sci. 10 (1975) 447–460.
[31] D.E. Koppel, Analysis of macromolecular polydispersity in intensity correlation spectroscopy. Method of cumulants, J. Chem. Phys. 57 (1972) 4814–4820.
[32] E.M. Goellner, J. Utermoehlen, R. Kramer, B. Classen, Structure of arabinogalactan from *Larix laricina* and its reactivity with antibodies directed against type-II-arabinogalactans, Carbohydr. Polym. 86 (2011) 1739–1744.
[33] S. Willför, R. Sjöholm, C. Laine, B. Holmbom, Structural features of water-soluble arabinogalactans from Norway spruce and Scots pine heartwood, Wood Sci. Technol. 36 (2002) 101–110.
[34] E. Nordmeier, Static and dynamic light-scattering solution behavior of pullulan and dextran in comparison, J. Phys. Chem. 97 (1993) 5770–5785.
[35] A.M. Striegel, J.D. Timpa, Molecular characterization of polysaccharides dissolved in *N*,*N*-dimethylacetamide-lithium chloride by gel-permeation chromatography, Int. J. Polym. Anal. Charact. 2 (1996) 213–220.
[36] H.A. Swenson, H.M. Kaustinen, J.J. Bachhuber, J.A. Carlson, Fractionation and characterization of larchwood arabinogalactan polymers A and B, Macromolecules 2 (1969) 142–145.
[37] G.L. Borgin, Molecular properties of water-soluble polysaccharides from western larch, J. Am. Chem. Soc. 71 (1949) 2247–2248.
[38] A.M. Striegel, J.D. Timpa, Molecular characterization of polysaccharides dissolved in *N*,*N*-dimethylacetamide-lithium chloride by gel-permeation chromatography, Carbohydr. Res. 267 (1995) 271–290.
[39] K. Parikka, A. Leppänen, L. Pitkänen, M. Reunanen, S. Willför, M. Tenkanen, Oxidation of polysaccharides by galactose oxidase, J. Agric. Food Chem. 58 (2010) 262–271.
[40] L. Pitkänen, P. Tuomainen, K.S. Mikkonen, M. Tenkanen, The effect of galactose side units and mannan chain length on the macromolecular characteristics of galactomannans, Carbohydr. Polym. 86 (2011) 1230–1235.
[41] T. Kato, T. Katsuki, A. Takahashi, Static and dynamic solution properties of pullulan in a dilute solution, Macromolecules 17 (1984) 1726–1730.
[42] B. Wittgren, K. Wahlund, Fast molecular mass and size characterization of polysaccharides using asymmetrical flow field-flow fractionation-multiangle light scattering, J. Chromatogr. A 760 (1997) 205–218.
[43] M. Leeman, K. Wahlund, B. Wittgren, Programmed cross flow asymmetrical flow field-flow fractionation for the size separation of pullulans and hydroxypropyl cellulose, J. Chromatogr. A 1134 (2006) 236–245.
[44] J.C. Giddings, Simplified nonequilibrium theory of secondary relaxation effects in programmed field-flow fractionation, Anal. Chem. 58 (1986) 735–740.

Supplementary information

Polysaccharide characterization by hollow-fiber flow field-flow fractionation with on-line multi-angle static light scattering and differential refractometry (HF5/MALS/DRI)

Leena Pitkänen, André M. Striegel*

Chemical Sciences Division, National Institute of Standards and Technology (NIST), 100 Bureau Drive, MS 8392, Gaithersburg, Maryland 20899

Demonstration of analyte transport through the HF5 fiber wall

That analyte transport through the HF5 fiber wall is an actual concern is shown by the analysis of two oligosaccharides, maltoheptaose and isomaltoheptaose, with the latter being an oligomer of pullulan. The solid lines in Figure S1 show the fractograms (or, more accurately, chromatograms), when the HF5 analysis was conducted in so-called "hydrodynamic chromatography mode" or "HDC mode" [S1, S2], i.e., using a flow of 0.2 mL min^{-1} in the absence of the cross-flow or focusing flow, with the oligosaccharides eluting via a hydrodynamic chromatography mechanism (the minuscule size difference between the maltoheptaose and isomaltoheptaose, as compared to the difference between their sizes and the PES fiber radius, precluded separation of the analytes from each other in HDC mode). In stark contrast, the dashed lines represent the fractogram of these same two analytes when the HF5 analysis was conducted employing the conditions described in Table 1. As can be seen from Figure S1, essentially all of the maltoheptaose and isomaltoheptaose samples went through the fiber during HF5 analysis, due to the much smaller size of these oligosaccharides (≤ 1 nm) [S3] as compared to the average pore size of the PES fibers (5 nm). This demonstrated that analyte transport through the HF5 fiber wall is a potential culprit for low analyte recovery when using this technique.

* To whom correspondence should be addressed. E-mail: andre.striegel@nist.gov

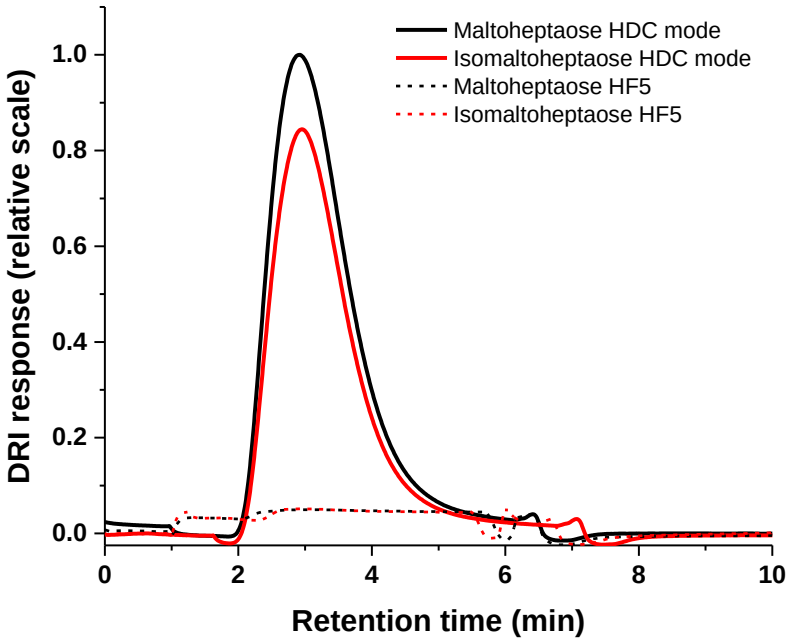

Figure S1. Maltoheptaose and isomaltoheptaose analyzed by HF5/MALS/DRI using flow conditions presented in Table 1 (solid lines) and in "HDC mode" without cross-flow or focus flow (dashed lines).

Effect of cross flow and focus flow on HF5 analyte recovery

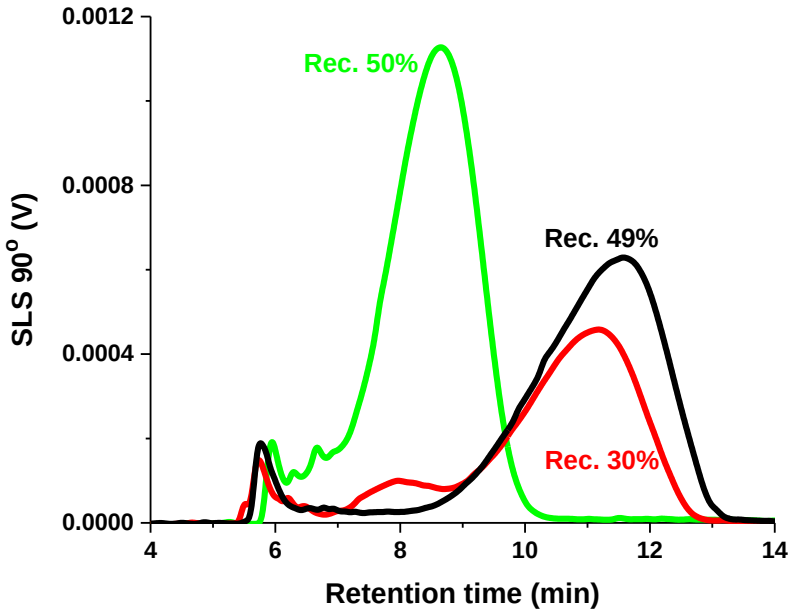

Figure S2. Static light scattering signals (SLS at 90°, in volts) and recovery values ("Rec.") for pullulan 212000 analyzed with different HF5 flow conditions. Black line represents the flow conditions presented in Table 1. Green line represents the conditions with lowered initial cross flow of 0.1 mL min^{-1} (otherwise the method is identical to the one in Table 1). The fractogram depicted in red was obtained using a lower focus flow of 0.2 mL min^{-1} (again, otherwise the method corresponds to that in Table 1). Recovery values of HF5 analyses were calculated from the DRI peak area and the $\partial n/\partial c$ value determined as described in **Section 2.5.**

References

[S1] A.M. Striegel, Hydrodynamic chromatography: packed columns, multiple detectors, and microcapillaries. Anal. Bioanal. Chem. 402 (2012) 77-81.
[S2] A.M. Striegel, A.K. Brewer. Hydrodynamic chromatography. Annu. Rev. Anal. Chem. 5 (2012) 15-34.
[S3] M.S. Motawia, I. Damager, C.E. Olsen, B.L. Møller, S.B. Engelsen, S. Hansen, L.H. Øgendal, R. Bauer, Comparative study of small linear and branched α-glucans using size exclusion chromatography and static and dynamic light scattering. Biomacromolecules 6 (2005) 143-151.